Field-induced ordering in a random-bond quantum spin ladder compound with weak anisotropy

G. S. Perren,[1] W. E. A. Lorenz,[1] E. Ressouche,[2] and A. Zheludev[1,*]
[1]*Laboratory for Solid State Physics, ETH Zürich, 8093 Zürich, Switzerland*
[2]*INAC, SPSMS, CEA Grenoble, 38054 Grenoble, France*

(Received 1 March 2018; revised manuscript received 14 May 2018; published 29 May 2018)

The field-induced quantum phase transitions in the disorder-free and disordered samples of the spin ladder material $(CH_3)_2CHNH_3Cu(Cl_{1-x}Br_x)_3$ are studied using magnetic calorimetry and magnetic neutron diffraction on single crystal samples. Drastically different critical indexes and correlation lengths in the high field phase are found for two different orientations of the applied field. It is argued that for a field applied along the crystallographic c axis, as in previous studies [T. Hong *et al.*, Phys. Rev. B **81**, 060410 (2010)], the transition is best described as an Ising transition in random field and anisotropy, rather than as a magnetic Bose glass to Bose condensate transition.

DOI: 10.1103/PhysRevB.97.174431

I. INTRODUCTION

Shortly after the realization that field-induced magnetic ordering in gapped quantum paramagnets can be viewed as a Bose-Einstein condensation (BEC) of magnons [1–3], a new research thrust was aimed at understanding the corresponding transition in disordered spin systems (for a review see Ref. [4]). The idea is that in the presence of disorder, the magnetic BEC state may be preceded by the magnetic analog of the long sought for Bose glass (BG) state [4–7]. The organic quantum spin ladder compound $(CH_3)_2CHNH_3Cu(Cl_{1-x}Br_x)_3$ (IPAX for short) was one of the first materials studied in this context [8–10]. Indeed, neutron scattering experiments under applied field revealed a BG-like gapless, magnetizable ("compressible") yet disordered magnetic state [8]. Most of the experimental work since was done on other disordered quantum magnets, such as $NiCl_{2-2x}Br_{2x} \cdot 4SC(NH_2)_2$ [7,11] and $(C_4H_{12}N_2)Cu_2(Cl_{1-x}Br_x)_6$ [12–14]. The main effort was aimed at understanding the critical exponents of the quantum phase transition between the magnetic BEC and BG phases. Of particular interest is the experimentally accessible exponent ϕ, which defines the field-temperature phase boundary $T_c = (H_c - H)^{\phi}$. The original work of Fisher *et al.* [5] predicted $\phi > 2$, as opposed to $\phi = 2/3$ in the absence of disorder. This theoretical result was later challenged by QMC calculations that suggested $\phi \approx 1.1$ [7], but were in turn contradicted by a later study consistent with Fischer's original arguments [15]. So far, experiments on materials like $NiCl_{2-2x}Br_{2x} \cdot 4SC(NH_2)_2$ [7,11,16] and $Tl_{1-x}K_xCuCl_3$ [17,18] have only added to the controversy, and the issue remains unresolved.

To date, there have been no systematic studies of critical exponents in the "original" BG-prototype compound IPAX. The parent material IPA-$CuCl_3$ crystallizes in a triclinic space group $P\bar{1}$ with $a = 7.78$ Å, $b = 9.71$ Å, $c = 6.08$ Å, $\alpha = 97.26°$, $\beta = 101.05°$, and $\gamma = 67.28°$ [19,20]. The magnetic properties are due to $S = 1/2$ Cu^{2+} ions that form weakly coupled two-leg ladders directed along the crystallographic a axis [21]. The ground state is a spin singlet. The magnetic excitation spectrum features a gap of $\Delta = 1.2$ meV and dispersive triplet excitations characteristic of a the spin ladder model [21,22]. Based on these neutron data, numerical modeling allowed us to determine the relevant exchange constants [23]. The magnon triplet is split into a singlet and doublet by 0.05 meV due to a very weak easy-axis anisotropy of exchange interactions [24,25]. The easy axis is roughly along the crystallographic b direction. The anisotropy is also manifest in the gyromagnetic tensor with $g_a = 2.05$, $g_b = 2.22$, and $g_c = 2.11$ [26]. The field-induced ordering transition occurs in $H_c \sim 9.7$ T [20]. The transition can to some extent be viewed as a BEC of magnons [27]. This picture is disrupted by the residual anisotropy which leads to an opening of a small gap in the ordered state [28]. In the Br-substituted compound IPAX the crystal structure is almost unchanged up to $x = 0.13$ [24]. The halogen substitution does not directly affect the magnetic Cu^{2+} ions, but instead randomizes the strengths of magnetic interactions.

Random magnetic interactions in IPAX leads to a Bose-glass-like precursor to the field-induced ordered phase [8–10]. However, from the start it was clear that the high-field phase itself is not exactly a magnetic BEC state. In particular, it unexpectedly shows only short-range magnetic order, with a history-dependent correlation length [8]. The present work addresses this unexplained behavior in a series of bulk measurements and additional neutron diffraction studies on the $x = 0.05$ and $x = 0$ systems. We show that the previously observed short-range order is directly linked to a weak magnetic anisotropy already present in the parent compound IPA-$CuCl_3$. We further argue that in the context of IPAX, and perhaps in most other quantum paramagnets with chemical disorder, it is more appropriate to speak of spin freezing in a random field environment, rather than of magnon condensation in a magnetic BG. In addition, we show that for an experimental geometry that minimizes anisotropy effects, the introduction of disorder does have a rather strong influence on the zone-boundary critical exponent.

*zhelud@ethz.ch; http://www.neutron.ethz.ch/

II. EXPERIMENTAL DETAILS

The present study was performed on the same fully deuterated IPA-$CuCl_3$ and $x = 0.05$ IPAX (IPAX-0.05 for short) single crystal samples as used in Refs. [27] and [8], respectively. Thermal-relaxation calorimetry was carried out on ∼1 mg fragments, using a Quantum Design 14 T PPMS with the ^{3}He-^{4}He dilution refrigerator insert. Typical relaxation times for a 2% differential were approximately 50 s. In field sweeps, the time needed for each 0.05 T field step was typically about 500 s. The data were collected in two field orientations. A close to axial geometry was realized with the magnetic fields **H** applied along the **b*** axis, which is conveniently perpendicular to a natural cleavage plane of the crystals. In this orientation the field is only ∼15° misaligned with the magnetic easy axis [26]. Alternatively, the field was applied along the crystallographic **c** direction, making it almost perpendicular to the anisotropy axis (transverse geometry).

A new series of neutron diffraction measurements on the D23 lifting-counter diffractometer at Institut Laue Langevin were performed on the $x = 0.05$ IPAX compound using a fully deuterated 150 mg single crystal. The magnetic field was applied along the **b** direction. This setting almost exactly realizes the axial geometry, in contrast to previous studies of Ref. [8] where the field was applied in the transverse direction. In our experiments, the sample environment was a 12 T cryomagnet with a dilution refrigerator insert. Diffraction was carried out using $\lambda = 1.218$ Å neutrons from a Cu-(200) monochromator.

III. RESULTS AND DATA ANALYSIS

A. Calorimetry

Typical magnetic $C(T)$ and $C(H)$ curves measured for IPAX and IPA-$CuCl_3$ are shown in Figs. 1 and 2, respectively. In the constant-field data, the Debye lattice contribution was measured in zero applied field and subtracted from the data shown. In all cases, a peak in the specific heat curve was taken as a signature of the onset of long-range order. For the disorder-free sample the lambda anomalies are perfectly sharp, but somewhat rounded in IPAX-0.05. In that case, the lambda anomaly is particularly broad in the transverse-field **H**∥**c** geometry, especially below $T \sim 1$ K.

To reconstruct the corresponding phase diagrams, the calorimetry data were analyzed with empirical "broadened power-law" fits for constant-field scans and "split-Lorentzian" fits for constant-T scans [12], shown as solid lines in Figs. 1 and 2, respectively. For the disorder-free system the transition was simply identified with the sharp maximum in the measured data. The results are shown in Fig. 3. The IPAX-0.05 phase boundary data measured in the transverse geometry using neutron diffraction in Ref. [8] are also shown. They appear to be consistent with the present calorimetric measurements, despite the larger scattering of data points. Also shown in Fig. 3 are data for the parent compound from Ref. [29] collected in the transverse-field geometry **H**∥**a**.

In order to estimate the exponents ϕ, the $C(H)$ phase-boundary data were analyzed using power-law fits. The common problem is choosing an appropriate fitting temperature range. An overly wide range may extend beyond the true quantum-critical regime, yielding incorrect power-law exponents. Shrinking the data range by limiting the maximum temperature T_{max} used for the fits, on the other hand, results in increased uncertainties on the fit parameters and eventually renders the result useless. The solution is to perform a series of fits over progressively shrinking temperature ranges, as described in Ref. [12]. The "optimal" minimal fitting range is such that further reducing T_{max} does not lead to a statistically significant change in the fitted values. In our case the fit parameters were ϕ, H_c, and an overall scale factor. The dependencies of the fitted value of ϕ on the temperature range used is plotted in Fig. 4. The results are very stable for all fitting ranges below the optimal $T_{max} = 0.6$ K for all measurements. This gives us confidence in the obtained exponents indeed correspond to the scaling behavior at QCP. The key parameters obtained for the optimal T_{max} are summarized in Table I. The corresponding fits are shown as solid lines in Fig. 3.

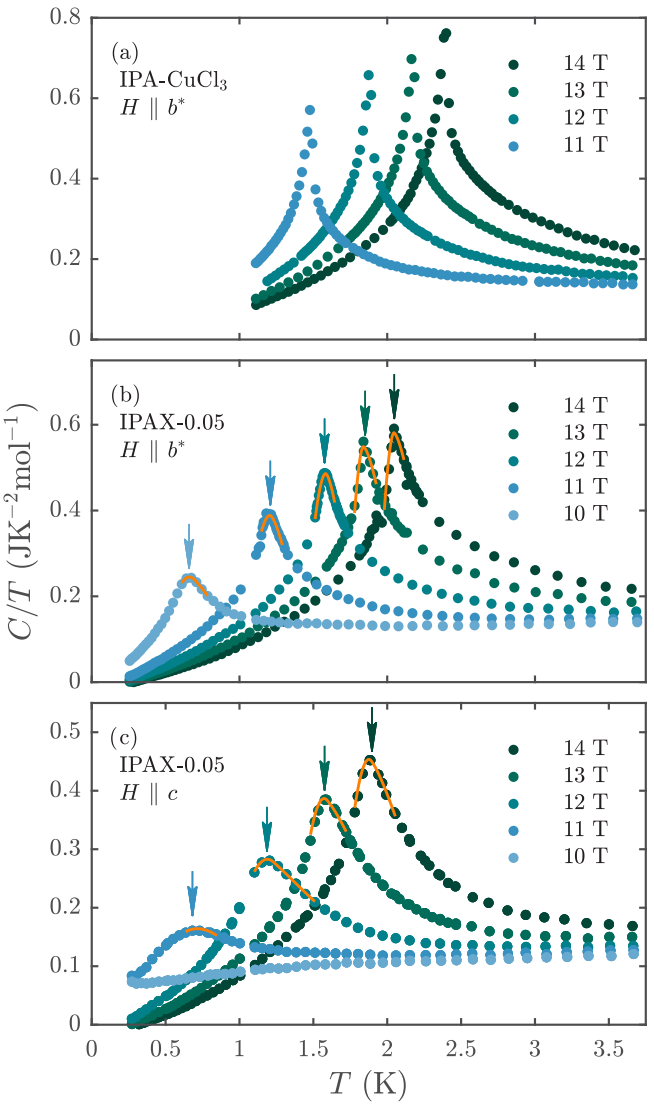

FIG. 1. Magnetic specific heat vs temperature measured in IPA-$CuCl_3$ (a) and IPAX (b) for a field applied almost parallel to the anisotropy axis, and IPAX in a field almost perpendicular to it (c). Solid lines are empirical fits to locate the maximum.

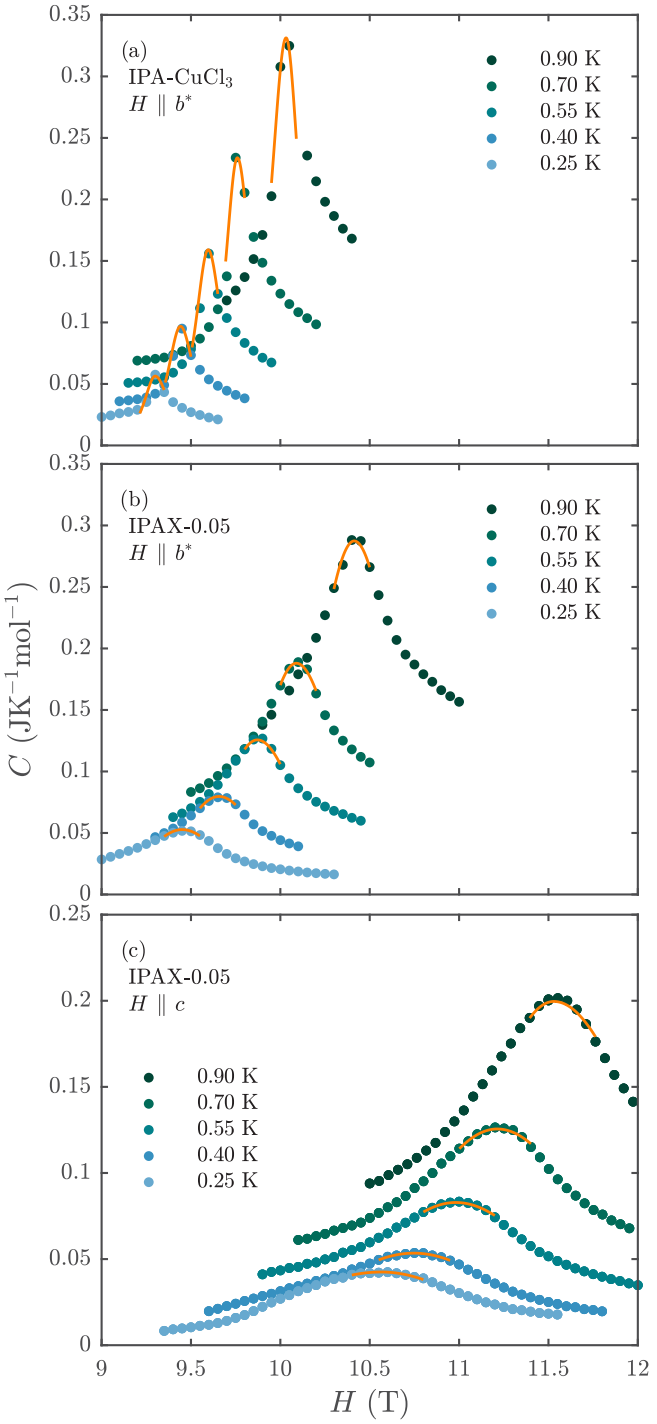

FIG. 2. Specific heat vs applied field, as measured in IPA-$CuCl_3$ (a) and IPAX (b) and (c). The field is almost parallel to the anisotropy axis in (a) and (b), and almost perpendicular to it în (c). Solid lines are empirical fits to locate the maximum.

B. Neutron diffraction

One of the more spectacular observations of the previous neutron study of IPAX-0.05 in the transverse-field geometry was the substantial and history-dependent broadening of the antiferromagnetic Bragg peaks in the high field phase [8]. A key result of the present work is that this effect, while still

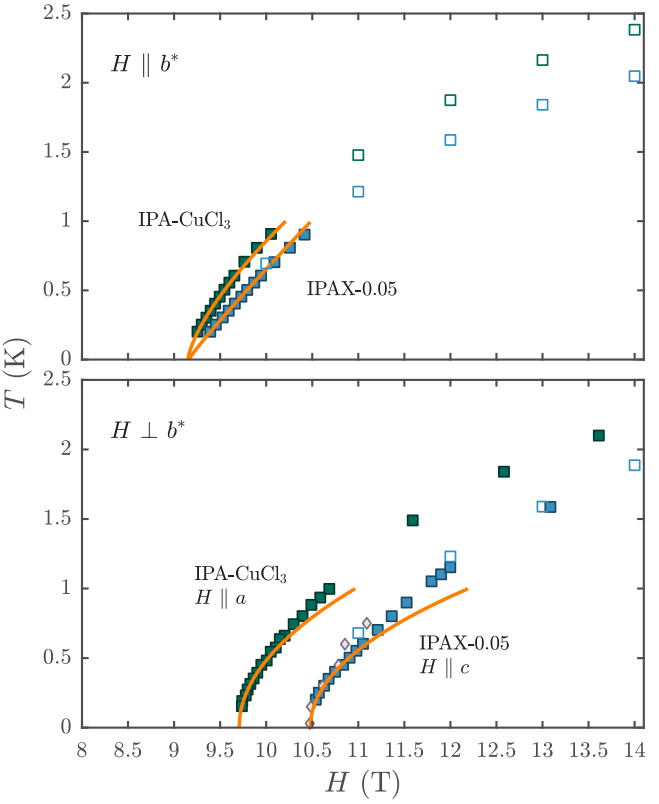

FIG. 3. Magnetic phase diagrams measured for IPA-$CuCl_3$ (top) and IPAX-0.05 (bottom) for magnetic fields applied almost parallel to the easy anisotropy axis (**b*** direction), and almost transverse to it. Solid and open squares are positions of specific heat maxima in constant-temperature and constant-field scans, respectively. Diamonds are neutron diffraction data from Ref. [8]. The **H**⊥**b*** data for the parent compound are from Ref. [29]. Solid lines are power-law fits as described in the text.

present, is drastically reduced in the almost axially symmetric configuration.

Figure 5 shows scans across the (0.5,0.5,0) magnetic reflections in the high-field phase of IPAX-0.05 for the magnetic field applied almost perpendicular [8] and almost parallel to the anisotropy axis (this work). These data were collected following either a field-cooling (FC) or zero-field cooling (ZFC) protocols. A Gaussian fit to instrumental resolution is in all cases shown as a dashed line. The resolution was determined by measuring the weak nuclear (1,1,0) Bragg contribution at

TABLE I. Parameters of power-law fits to the calorimetric phase boundary data in a temperature range $T < T_{max} = 0.6$ K. The analysis for IPA-$CuCl_3$ in **H**⊥**b*** was based on data from Ref. [29].

	ϕ	H_c (T)
H∥**b***:		
IPA-$CuCl_3$	0.71(1)	9.15(1)
IPAX-0.05	0.93(1)	9.16(1)
H⊥**b***:		
IPA-$CuCl_3$ (**H**∥**c**)	0.50(1)	9.99(1)
IPAX-0.05 (**H**∥**a**)	0.49(1)	10.48(1)

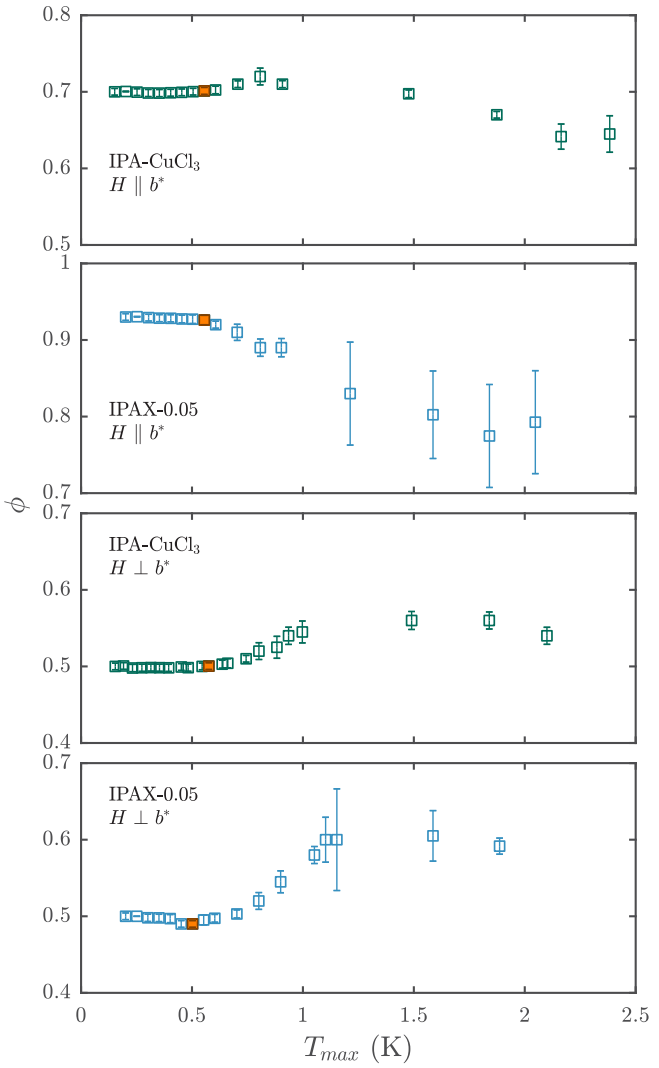

FIG. 4. Shrinking-fit-window analysis of the measured phase boundaries. The plots show the least-squares fitted values of the phase boundary exponent ϕ vs the temperature range used for the fit. The other two fit parameters H_c and an overall scaling factor are not shown.

(0.5,0.5,0) due to $\lambda/2$ beam contamination. One immediately sees that the broadening and associated reduction in peak intensity of the ZFC peaks compared to FC ones is considerably smaller in the close to axial setting. In fact, in that case the peaks are almost resolution limited regardless of cooling protocol.

To quantify this observation we analyzed all the measured scans using Lorentzian-squared profiles [30] numerically convoluted with the instrument resolution. The fits are show in Fig. 5 as solid lines and allow us to extract the correlation length ξ, tabulated in Table II.

For a transverse field, the history-dependent short-range order in IPAX-0.05 is also manifest in a hysteretic field and temperature dependencies of the diffraction peak height [8]. Such a hysteresis measurement for the close to axial geometry is shown in Fig. 6. The sample was first cooled in zero field to $T = 50$ mK, then the magnetic field was raised to $H = 11.5$ T. Following that, the sample was warmed up to above the ordering temperature at a constant field, and the trajectory

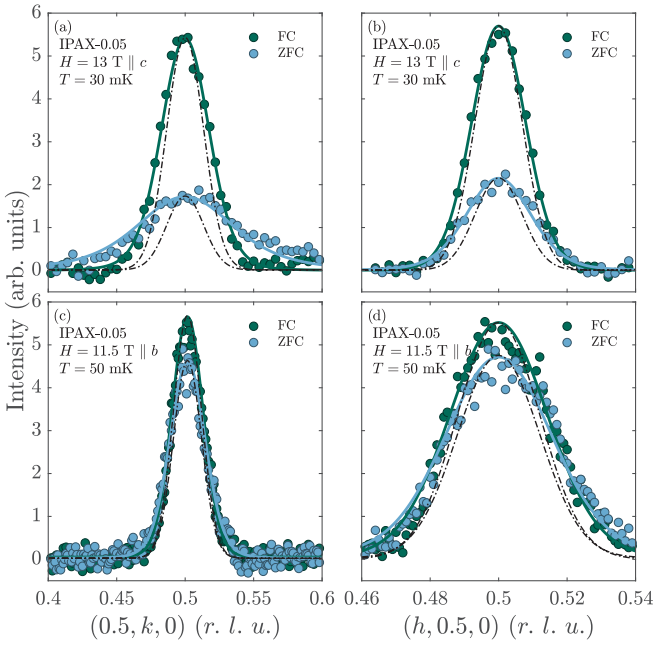

FIG. 5. Magnetic (0.5,0.5,0) Bragg peaks measured in IPAX-0.05 for a magnetic field applied almost perpendicular [(a) and (b)] and almost parallel [(c) and (d)] to the easy anisotropy axis. The data were collected using field-cooling (FC, open symbols) and zero-field-cooling (ZFC, closed symbols) protocols. The dash-dot lines represent experimental Gaussian resolution that was measured as described in the text. Solid lines are fits to the data of Lorentzian-squared functions folded with the experimental resolution. The experimental data in (a) and (b) are from Ref. [8].

was reversed. While the hysteresis is clearly observed, it is considerably smaller than for a transverse-field orientation [8]. Overall, in the observed behavior the close to axial geometry is similar to that previously seen in $(C_4H_{12}N_2)Cu_2(Cl_{1-x}Br_x)_6$, but with an even smaller hysteretic effect [12].

IV. DISCUSSION

The first thing to note is the clear differences in behavior of the disorder-free system in the two orientations. In agreement with Ref. [28], for the off-axial field, BEC of magnons is a poor description for the criticality of the transition. The measured

TABLE II. Magnetic correlation length measured in IPAX-0.05 for a magnetic field applied almost perpendicular [8] and almost parallel to the anisotropy axis, in field-cooled and zero-field-cooled samples. The values are obtained from Lorentzian-squared fits to the diffraction data, as described in the text.

	ξ_b (Å)	ξ_c (Å)
$\perp$ geometry [8]:		
FC	30(4)	94(7)
ZFC	8.3(1)	50(5)
$\parallel$ geometry:		
FC	97(6)	83(4)
ZFC	97(6)	83(4)

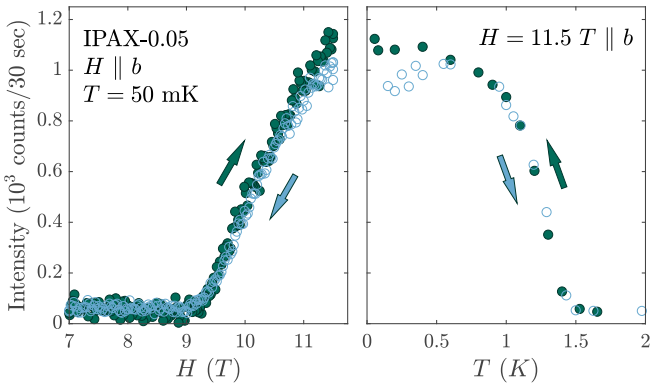

FIG. 6. Peak intensity of the (0.5,0.5,0) Bragg reflection measured in IPAX-0.05 for a magnetic field applied almost parallel to the easy anisotropy axis. The measurements are performed following zero-field-cooling the sample, and through an isothermal field ramping at low temperature, warming to above the transition temperature, field-cooling and an isothermal ramping down of the applied field. The observed history dependence is much smaller than previously seen in the transverse-field geometry [8].

value of the phase boundary exponent is in better agreement with that of the 3+1 dimensional Ising model ($\phi = 1/2$, since $z = 1$ and $\nu = 1/2$ at the upper critical dimension) then with $\phi = 2/3$ expected for a 3+2 dimensional BEC of magnons (mean field) [1]. That the material behaves as an Ising system for $\mathbf{H}\perp\mathbf{b}$ at $T \lesssim 1$ K is, in retrospect, not surprising, since the anisotropy in the (a^*,b^*) plane is itself of the order of 0.5 K [24,25]. Similar residual anisotropy has been a complication for most examples of magnon BEC in quantum magnets [31], including $TlCuCl_3$ [32,33]. Moreover, in IPA-$CuCl_3$, due to a low crystal symmetry, a truly axially symmetric geometry cannot be perfectly restored by a choice of field direction. Nevertheless, applying a field close to the principal axis of anisotropy seems to approximate the BEC scenario reasonably well, at least as far as the measured critical exponent is concerned.

For the disordered material, the short-range ordering and history dependence is clearly strongest in the transverse-field geometry. Therefore, it must be interpreted as an effect of disorder not on a BEC of magnons, but on a transition that is in the Ising universality class. The chemical Cl/Br disorder in IPAX will have several consequences for the magnetic Hamiltonian. First, the strength of antiferromagnetic interactions will be affected due to variances in Cu-Cl and Cu-Br covalency strengths and distortions of superexchange bond angles. This type of disorder is exactly what translates into a random potential for bosons, as envisioned in the magnetic Bose glass picture [4]. In addition however, distortions of the local Cu^{2+} crystallographic environments will lead to a random component to the magnetic ion's gyromagnetic tensor. In the presence of a uniform external magnetic field, this will effectively generate a *random spin field* in the sample. Its component along the applied uniform field couples to magnetization, i.e., magnon density. Thus it adds to the random potential for magnons. However, the transverse component of the spin field is directly coupled to the order parameter of the phase transition, namely the transverse magnetization. Such random fields are known to have drastic effects on phase transitions [34]. The third effect of chemical disorder is random two-ion (exchange) anisotropy. In the presence of a uniform external field a random anisotropy becomes again equivalent to a random field, with all the same consequences [35]. We conclude that for a field applied perpendicular to the principal anisotropy axis the phase transition in IPAX is to be viewed as that in a random field and random bond (RF+RB) Ising transition, and surely not as a BEC to BG transition, as implied in Ref. [8].

The ideal RF Ising model is known to order in three dimensions [34]. The quantum and thermodynamic phase transitions are, in fact, governed by the same fluctuationless fixed point [36]. Nevertheless, the actual behavior observed in prototype materials such as diluted AFs in a uniform field is quite different [37,38]. Rather than showing long-range order, these systems, of which $Mn_xZn_{1-x}F_6$ is perhaps the best known example [37], go through a freezing transition. Below that point there is static but only short-range order. The system breaks up into microscopic domains. The domain size is history dependent, but can only increase as long as one does not exit into the paramagnetic phase. There is also no temporal relaxation of domain size. This anomalous behavior has been attributed to the simultaneous presence of RF and RB [39]. This situation exactly corresponds to IPAX. Indeed, in the transverse-field configuration we observe almost exactly the type of behavior as seen in $Mn_xZn_{1-x}F_6$ at a fixed random-field strength.

A feature that is somewhat special to IPAX is the anisotropy of the short-range static correlations in the high-field phase in ZFC experiments in off-axial geometry (see Fig. 5 and Table II). Undoubtedly the effect is related to the quasi-one-dimensional nature of the material. Below H_c, at temperatures small compared to the gap Δ, the equal-time (dynamic) correlations are fairly well established along the chain direction. The corresponding correlation length is $\xi \sim u/\Delta$, where u is the spin wave velocity. For the parent compound IPA-$CuCl_3$ this amounts to about three lattice repeats or 20 Å [21]. This sets the *lower* limit on the length of static correlations that freeze in the high field phase in IPAX. In contrast, below H_c the equal-time correlations between ladders in IPA-$CuCl_3$ are virtually nonexistent, due to the interladder interactions being much smaller than the quantum spin gap. As a result, no such intrinsic lower limit inherited from the disorder-free system exists for b-axis static correlations in IPAX, and they are entirely due to random field effects. Indeed, for the ZFC experiments in the off-axial geometry we find a correlation length comparable to a single lattice spacing.

The pinning of domains is governed by the width of the domain walls, i.e., by the relative magnitude of anisotropic vs axially symmetric magnetic interactions [39]. For IPAX, the off-axial component of anisotropy is weakest in the close to axial geometries. In these configurations the pinning and resulting history-dependent behavior can thus expected to be much weaker than in the transverse-field case. This is totally consistent with our observations. In IPAX-0.05 in a field applied almost along the anisotropy axis, the small hysteretic effects and internal linewidth aside, we observe what almost is a long-range-ordered phase. Perhaps by coincidence, adding disorder has almost no effect on the critical field H_c in this case. Nonetheless, the phase boundary is significantly modified. The

measured critical exponent is very similar to that observed under similar conditions in $(C_4H_{12}N_2)Cu_2(Cl_{1-x}Br_x)_6$ [12] and $NiCl_{2-2x}Br_{2x} \cdot 4SC(NH_2)_2$ [7]. Regardless of whether $\phi \sim 1$ is indeed the correct critical exponent for the BG to BEC transition or not [15], and whether that scenario is at all relevant for IPAX-0.05 in the close-to-axial configuration, experimentally it seems to be a rather common situation in disordered magnets. Interestingly, for a transverse-field configuration the phase boundary critical exponent appears to be unchanged by the presence of disorder.

The "unwanted" random anisotropy and random fields may have an even bigger impact on quantum phase transitions in very strongly one-dimensional systems with bond disorder, such as spin chains and ladders with chemical randomness. Here (unlike in IPA-$CuCl_3$ where interladder coupling is actually substantial) even in the absence of disorder the saturation moment is only a tiny fraction of its classical value. Disorder of any kind is expected to have a huge effect on the field-induced transition, the critical exponents, and the structure of the ordered phase. As has been demonstrated in the frustrated spin chain compounds $H_8C_4SO_2 \cdot Cu_2(Cl_{1-x}Br_x)_4$, even the transition itself may become entirely suppressed [40]. A different family of materials where this issue can be addressed without the complication of geometric frustration are the bond-disordered spin ladders $(Hpip)_2Cu(Cl_x,Br_{1-x})_4$. These compounds have experimentally accessible transition fields, and the effect of randomness of Br substitution on the thermodynamic properties and magnetic excitations is well established [41]. A careful look at the effect of chemical disorder on the critical exponents of the field-induced quantum transition may be the next step.

V. CONCLUSION

In summary, random anisotropy and random field effects can never be fully disregarded in field-induced phase transitions in materials with chemical disorder, even if the latter does not involve the magnetic ions directly. Nonetheless, the bond-disorder related increase of the crossover exponent ϕ to about unity from its $\phi = 2/3$ value in the ideal BEC case can still be observed in geometries in which these effects are minimized.

ACKNOWLEDGMENT

This work was partially supported by the Swiss National Science Foundation, Division II.

[1] T. Giamarchi and A. M. Tsvelik, Coupled ladders in a magnetic field, Phys. Rev. B **59**, 11398 (1999).
[2] T. M. Rice, To condense or not to condense, Science **298**, 760 (2002).
[3] T. Giamarchi, Ch. Rüegg, and O. Tchernyshev, Bose–Einstein condensation in magnetic insulators, Nat. Phys. **4**, 198 (2008).
[4] A. Zheludev and T. Roscilde, Dirty-boson physics with magnetic insulators, C. R. Phys. **14**, 740 (2013).
[5] M. P. A. Fisher, P. B. Weichman, G. Grinstein, and D. S. Fisher, Boson localization and the superfluid-insulator transition, Phys. Rev. B **40**, 546 (1989).
[6] R. Yu, S. Haas, and T. Roscilde, Universal phase diagram of disordered bosons from a doped quantum magnet, Europhys. Lett. **89**, 10009 (2010).
[7] R. Yu, L. Yin, N. S. Sullivan, J. S. Xia, C. Huan, A. Paduan-Filho, N. F. Oliveira Jr., S. Haas, A. Steppke, C. F. Miclea, F. Weickert, R. Movshovich, E.-D. Mun, B. L. Scott, V. S. Zapf, and T. Roscilde, Bose glass and Mott glass of quasiparticles in a doped quantum magnet, Nature (London) **489**, 379 (2012).
[8] T. Hong, A. Zheludev, H. Manaka, and L.-P. Regnault, Evidence of a magnetic Bose glass in $(CH_3)_2CH\,NH_3Cu(Cl_{0.95}Br_{0.05})_3$ from neutron diffraction, Phys. Rev. B **81**, 060410 (2010).
[9] H. Manaka, A. V Kolomiets, and T. Goto, Disordered States in IPA-$Cu(Cl_{1-x}Br_x)_3$ Induced by Bond Randomness, Phys. Rev. Lett. **101**, 077204 (2008).
[10] H. Manaka, H. A. Katori, O. V. Kolomiets, and T. Goto, Bose-glass state in one-dimensional random antiferromagnets, Phys. Rev. B **79**, 092401 (2009).
[11] E. Wulf, D. Hüvonen, J.-W. Kim, A. Paduan-Filho, E. Ressouche, S. Gvasaliya, V. Zapf, and A. Zheludev, Criticality in a disordered quantum antiferromagnet studied by neutron diffraction, Phys. Rev. B **88**, 174418 (2013).
[12] D. Hüvonen, S. Zhao, M. Månsson, T. Yankova, E. Ressouche, C. Niedermayer, M. Laver, S. N. Gvasaliya, and A. Zheludev, Field-induced criticality in a gapped quantum magnet with bond disorder, Phys. Rev. B **85**, 100410 (2012).
[13] D. Hüvonen, S. Zhao, G. Ehlers, M. Månsson, S. N. Gvasaliya, and A. Zheludev, Excitations in a quantum spin liquid with random bonds, Phys. Rev. B **86**, 214408 (2012).
[14] D. Hüvonen, G. Ballon, and A. Zheludev, Field-concentration phase diagram of a quantum spin liquid with bond defects, Phys. Rev. B **88**, 094402 (2013).
[15] Z. Yao, K. P. C. da Costa, M. Kiselev, and N. Prokof'ev, Critical Exponents of the Superfluid Bose-Glass Transition in Three Dimensions, Phys. Rev. Lett. **112**, 225301 (2014).
[16] E. Wulf, D. Hüvonen, R. Schönemann, H. Kühne, T. Herrmannsdörfer, I. Glavatskyy, S. Gerischer, K. Kiefer, S. Gvasaliya, and A. Zheludev, Critical exponents and intrinsic broadening of the field-induced transition in $NiCl_2 \cdot 4SC(NH_2)_2$, Phys. Rev. B **91**, 014406 (2015).
[17] F. Yamada, H. Tanaka, T. Ono, and H. Nojiri, Transition from Bose glass to a condensate of triplons in $Tl_{1-x}K_xCuCl_3$, Phys. Rev. B **83**, 020409 (2011).
[18] A. Zheludev and D. Hüvonen, Comment on "Transition from Bose glass to a condensate of triplons in $Tl_{1-x}K_xCuCl_3$", Phys. Rev. B **83**, 216401 (2011).
[19] H. Manaka, I. Yamada, and K. Yamaguchi, Ferromagnetic-dominant alternating Heisenberg chains with ferromagnetic and antiferromagnetic interactions formed in $(CH_3)_2CH\,NH_3CuCl_3$, J. Phys. Soc. Jpn. **66**, 564 (1997).
[20] H. Manaka, I. Yamada, Z. Honda, H. Aruga Katori, and K. Katsumata, Field-induced magnetic long-range order in the ferromagnetic-antiferromagnetic alternating Heisenberg chain

system $(CH_3)_2CH\ NH_3CuCl_3$ observed by specific heat measurements, J. Phys. Soc. Jpn. **67**, 3913 (1998).

[21] T. Masuda, A. Zheludev, H. Manaka, L.-P. Regnault, J.-H. Chung, and Y. Qiu, Dynamics of Composite Haldane Spin Chains in IPA-$CuCl_3$, Phys. Rev. Lett. **96**, 047210 (2006).

[22] A. Zheludev, V. O. Garlea, T. Masuda, H. Manaka, L.-P. Regnault, E. Ressouche, B. Grenier, J.-H. Chung, Y. Qiu, K. Habicht, K. Kiefer, and M. Boehm, Dynamics of quantum spin liquid and spin solid phases in IPA-$CuCl_3$ under an applied magnetic field studied with neutron scattering, Phys. Rev. B **76**, 054450 (2007).

[23] T. Fischer, S. Duffe, and G. S. Uhrig, Microscopic model for Bose-Einstein condensation and quasiparticle decay, Europhys. Lett. **96**, 47001 (2011).

[24] H. Manaka, I. Yamada, M. Hagiwara, and M. Tokunaga, High-field and high-frequency ESR study of the Haldane state formed in the ferromagnetic and antiferromagnetic alternating Heisenberg chain system $(CH_3)_2CHNH_3CuCl_3$, Phys. Rev. B **63**, 144428 (2001).

[25] B. Náfrádi, T. Keller, H. Manaka, A. Zheludev, and B. Keimer, Low-Temperature Dynamics of Magnons in a Spin-1/2 Ladder Compound, Phys. Rev. Lett. **106**, 177202 (2011).

[26] H. Manaka, K. Masamoto, and S. Maehata, Three-dimensional observation of composite Haldane spin chains in IPA-$CuCl_3$ by electron spin resonance using a two-rotation-axis goniometer, J. Phys. Soc. Jpn. **76**, 023002 (2007).

[27] V. O. Garlea, A. Zheludev, T. Masuda, H. Manaka, L.-P. Regnault, E. Ressouche, B. Grenier, J.-H. Chung, Y. Qiu, K. Habicht, K. Kiefer, and M. Boehm, Excitations from a Bose-Einstein Condensate of Magnons in Coupled Spin Ladders, Phys. Rev. Lett. **98**, 167202 (2007).

[28] Z. Y. Zhao, B. Tong, X. Zhao, L. M. Chen, J. Shi, F. B. Zhang, J. D. Song, S. J. Li, J. C. Wu, H. S. Xu, X. G. Liu, and X. F. Sun, Thermal conductivity of IPA-$CuCl_3$: Evidence for ballistic magnon transport and the limited applicability of the Bose-Einstein condensation model, Phys. Rev. B **91**, 134420 (2015).

[29] H Tsujii, Y H Kim, Y Yoshida, Y Takano, T P Murphy, K Kanada, T Saito, A Oosawa, and T Goto, Magnetic phase diagram of the $s = 1/2$ antiferromagnetic ladder $(CH_3)_2CHNH_3CuCl_3$, J. Phys.: Conf. Ser. **150**, 042217 (2009).

[30] In Ref. [8] the correlation length was extracted in Lorentzian fits. However, using a Lorentzian squared instead is more justified. It has the simple physical meaning of being the Fourier transform of an exponential correlation function in real space. Also, unlike that of the Lorentzian, its integral over reciprocal space is finite.

[31] R. Dell'Amore, A. Schilling, and K. Krämer, $U(1)$ symmetry breaking and violated axial symmetry in $TlCuCl_3$ and other insulating spin systems, Phys. Rev. B **79**, 014438 (2009).

[32] V. N. Glazkov, A. I. Smirnov, H. Tanaka, and A. Oosawa, Spin-resonance modes of the spin-gap magnet $TlCuCl_3$, Phys. Rev. B **69**, 184410 (2004).

[33] A. K. Kolezhuk, V. N. Glazkov, H. Tanaka, and A. Oosawa, Dynamics of an anisotropic spin dimer system in a strong magnetic field, Phys. Rev. B **70**, 020403 (2004).

[34] Y. Imry and S.-K. Ma, Random-Field Instability of the Ordered State of Continuous Symmetry, Phys. Rev. Lett. **35**, 1399 (1975).

[35] S. Fishman and A. Aharony, Random field effects in disordered anisotropic antiferromagnets, J. Phys. C: Solid State Phys. **12**, L729 (1979).

[36] T. Senthil, Properties of the random-field Ising model in a transverse magnetic field, Phys. Rev. B **57**, 8375 (1998).

[37] R. J. Birgeneau, R. A. Cowley, G. Shirane, and H. Yoshizawa, Temporal Phase Transition in the Three-Dimensional Random-Field Ising Model, Phys. Rev. Lett. **54**, 2147 (1985).

[38] R. J. Birgeneau, H. Yoshizawa, R. A. Cowley, G. Shirane, and H. Ikeda, Random-field effects in the diluted two-dimensional ising antiferromagnet $Rb_2Co_{0.7}Mg_{0.3}F_4$, Phys. Rev. B **28**, 1438 (1983).

[39] T. Nattermann and I. Vilfan, Anomalous Relaxation in the Random-Field Ising Model and Related Systems, Phys. Rev. Lett. **61**, 223 (1988).

[40] E. Wulf, S. Mühlbauer, T. Yankova, and A. Zheludev, Disorder instability of the magnon condensate in a frustrated spin ladder, Phys. Rev. B **84**, 174414 (2011).

[41] S. Ward, P. Bouillot, H. Ryll, K. Kiefer, K. W. Kramer, Ch. Ruegg, C. Kollath, and T. Giamarchi, J. Phys.: Condens. Matter **25**, 014004 (2013).